Algorithm based Drive Design for a Ventricular Assist Device

André Pohlmann, Marc Leßmann and Kay Hameyer
RWTH Aachen University, Institute of Electrical Machines
Schinkelstraße 4, 52056 Aachen, Germany
E-mail: Andre.Pohlmann@iem.rwth-aachen.de

Abstract - **In industrialized countries, cardiovascular diseases are the major cause of death. One therapy option for terminal heart failure is heart transplantation. Due to the limited number of human donor hearts, many patients die while waiting for a donor organ. One possibility to sustain the patients' life are Ventricular Assist Devices (VAD), which support the human heart to achieve a sufficient perfusion of the body. The main components of a VAD are its blood pump and its drive unit, which is designed in this paper. For the drive design the most important constraints are dimensions and electric losses while providing sufficient torque for the pump unit. Therefore, the Differential Evolution Algorithm (DEA) in combination with Finite Element (FE) simulations is applied to achieve an optimum electromagnetic drive design under the predefined constraints.**

I. INTRODUCTION

According to the World Health Organization cardiovascular diseases are the major cause of death in industrialized countries [1]. One therapy option of patients, suffering from terminal heart failure, is heart transplantation, which is dependent on the available number of donor hearts. For this reason many patients die while waiting for a donor organ [2]. In order to sustain the patients' life, Ventricular Assist Devices (VAD) can mechanically support the human heart to achieve a sufficient perfusion of the body. There are two therapy strategies called bridge to transplant and bridge to recovery. In the last strategy the heart might recover, because the VAD unloads it. Fig. 1 shows the schematic of a radial flow VAD. The pump unit contains parts of the housing for the flow guiding and an impeller, while the drive consists of a rotor, made of neodymium iron boron (NdFeB) permanent magnets, a hydrodynamic axial bearing and the stator. This arrangement yields the axial flux permanent magnet brushless DC (BLDC) motor.

The general design of the BLDC drive is presented in Fig. 2, while the optimized specifications are determined by the Differential Evolution Algorithm (DEA) in the next section. The rotor consists of 16 alternating axial magnetized
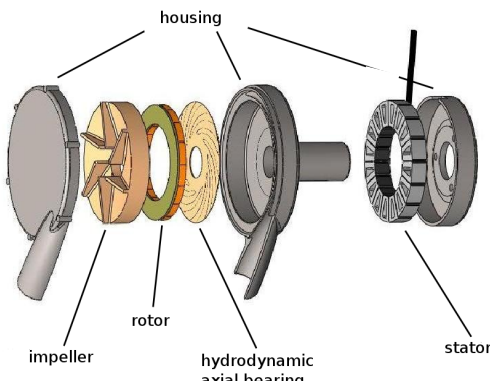
Fig. 1: Schematic of a radial flow VAD.
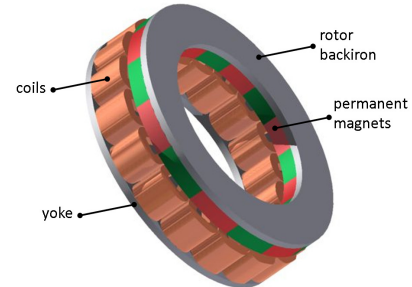
Fig. 2: CAD drawing of the general VAD drive design.

magnets with a remanent induction of 1.4 T at 20 ˚C, which are attached to the rotor backiron. Due to the axial flux direction, the backiron as well as the stator yoke is made of solid ferromagnetic steel (9S20) with a saturation induction 1.7 T. Hence, eddy currents occur there. The stator coils are hand wounded with a rectangular copper wire. For the following drive design the copper fill factor is estimated to 60%. The hydrodynamic bearing relies on a thin film of blood and therefore works without contact and passive. It consists of a compound disc with integrated flow channels (s. Fig. 1), which design influences the stiffness and acceptable forces. For the given design an axial force of 9 N can be compensated. The air gap between the top of the stator coils ant the bottom of the rotor magnets amounts to 1 mm.

II. DESIGN OBJECTIVES

The design objectives are given in Table 1. While the nominal speed and torque are required for the pump unit to generate a sufficient perfusion of the human body, the overall efficiency of the VAD is maximized for the maximum allowed axial force. In order to avoid blood damage by overheating, caused by copper losses, the electric losses have to be minimized. In this paper the rotor dimensions are given and the stator dimensions are limited for a minimal invasive implantation of the device.

The attracting axial force $\vec{F}_{axial}$ between the stator and the rotor can be calculated by applying the equation

$$\vec{F}_{axial} = \frac{B^2 \cdot A}{2 \cdot \mu_0} \cdot \vec{e}_{axial} \ , \tag{1}$$

with the induction B, the cross section area A of the induction and the permeability of the vacuum μ_0. As the magnetic field H is linked with the induction B by the product of the relative permeability μ_r and the vacuum permeability μ_0,

$$B = \mu_0 \cdot \mu_r \cdot H \ , \tag{2}$$

TABLE 1: DESIGN PARAMETERS

design objectives	
nominal speed	2500 rpm
nominal torque	12 mNm
max. axial force	9 N
max stator height	< 7mm
max. outer radius	< 19.5 mm

the axial force can be adjusted by varying the height of the ferromagnetic stator teeth, which relative permeability is higher when compared to the permeability of air. This results in coils, which are partially filled with ferromagnetic iron and air, to design a drive with a good efficiency. The radial component of the force $\vec{F}_{rad}$ is calculated by the Lorentz force equation

$$\vec{F}_{rad} = I \cdot (\vec{l} \times \vec{B}) \cdot \vec{e}_{rad} \,, \tag{3}$$

with the current supply I and the active wire length l of the coils. As the resulting torque is linked with the radial force, both the torque and the axial force are dependent on the induction B of the motor. Due to the significant flux leakage and the rotational movement of the drive, transient and non linear Finite Element (FE) simulations are required to determine the distribution of the induction in the motor. The results, shown in Fig. 3, have been obtained by a solver from the FE software package iMOOSE, which is developed at the Institute of Electrical Machines of the RWTH Aachen University [5]. In summary the design objectives have to be within the given dimensions, generate at least the required torque and adjust the axial force to 9N.

III. DIFFERENTIAL EVOLUTION ALGORITHM

In order to achieve an optimum drive design the Differential Evolution Algorithm (DEA) is applied for the drive design according to the introduced objectives [3]. The DEA is a generic and population based optimization algorithm introduced in [4], [5]. At the beginning the constraints and the design parameters are set. As the design parameters are initialized with random values, their lower and upper limit are defined as well. Then a first generation of computer models is created. The number D of models equals ten times the amount of the design parameters.

As explained before a FE simulation is required for each model to obtain the axial forces and resulting torque. Due to the rotational movement the reluctance force between stator and rotor vary, requiring a transient simulation of 15 deg. mechanically (mech.), corresponding to 120 deg. electrically (el.) for the torque and axial force determination. No further steps are required because of the drive symmetry.

In order to speed up the algorithm based design process, the simulations are performed assuming linear material characteristics here. If the required torque can be generated, the resulting ohmic losses $P_{l,calc}$ and axial forces $F_{axial,calc}$ are simulated. Otherwise the model is reinitialized with a different design parameter set to ensure the desired number of computer models for one generation and the convergence of the DEA process. For a fair comparison each model is virtually
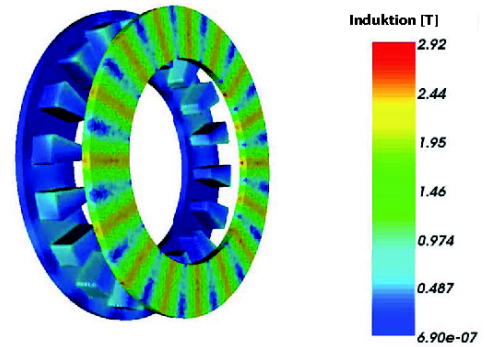
Fig. 3: Distribution of the induction in the BLDC drive

supplied with a current linkage Θ of 50 A in the simulation. Therefore, the generated torque as well as the resulting losses depend on the drive geometry. By applying the cost function CF,

$$CF = a \cdot \exp(\frac{P_{l,calc}}{P_{l,\max}}) + b \cdot \exp(\frac{\left|F_{axial,calc} - F_{axial,\max}\right|}{F_{axial,\max}}) \,, \tag{4}$$

the quality of each model is determined in terms of losses and forces. In order to give priority either to the losses or to the resulting axial forces during the optimization process the parameters a and b are initialized with a value between 0 and 1, while the sum of a and b equals to 1 [6]. For this reason the best model in theory has no losses, while the axial force amounts to 9 N. In this way a list, containing the hierarchic order of the best models is generated. Based on the best model of this population a new generation and as well a second list is created. The two lists are merged by comparing the quality of each model and only keeping the best ones. After several iterations this process yields the optimum drive design with a high efficiency and an axial force of 9 N when the algorithm is converging.

IV. SIMULATION RESULTS RESULTS

As adjustments in the introduced calculation chain were required to achieve a tolerable computation time and to ensure the convergence of the DEA, the design process was started three times. By learning from the previous run, the amount of design parameter was reduced to four of the final one, which results are shown in Fig. 4. The best member yields a cost function value of 1.25 (a). After iteration number 15 the DEA improves the drive design only marginally, which is explained with the converging of the DEA. In (b) the mean distance to the cost function is presented, which is calculated by the mean value of the cost function of all models of one generation. At the beginning the mean distance is really high, but improves as the design parameter of the generation n+1 are based on the design parameters of the best model of generation n. At the end the quality of all models are really close to each other, proofing the converging of the DEA. As the air gap, which is included in the maximum stator height, and the thickness of the stator yoke ring are both 1 mm, the coil height is close to its maximum value of 5 mm (f). Hence, the ratio between the stator teeth and coil height (e) sums up to 73 %. According
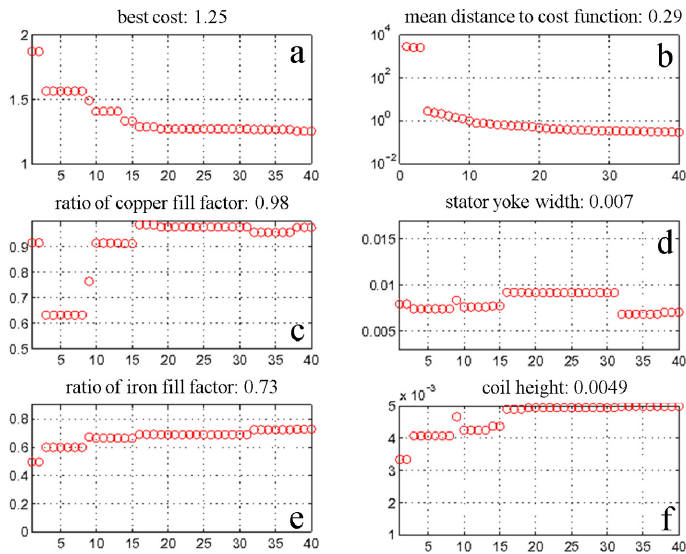
Fig. 4: Results of the DEA drive design process.

to a previous DEA run, the outer radius converges against its maximum boundary of 18.5 mm. Together with the stator yoke width the average coil length is defined. For a yoke width of 7 mm (d), the required torque is generated at lowest possible losses. The best member yielded an axial attracting force of 9.12 N for linear FEM simulations.

Due to the occurring stray flux and the non linear characteristic of the ferromagnetic iron and permanent magnets, non linear FEM simulations have been performed, to validate the drive design of the best member, obtained from the DEA. Hence, the ohmic losses and the mean axial force amount to 0.66 W and 9.01 N respectively.

In Fig. 5 the axial force and the generated torque characteristic is shown. For the VAD drive a field oriented control with pulse current is applied. Therefore the current is commutated every 60 deg. (el.) corresponding to 7.5 deg. (mech.). At 6 deg. the axial force reaches its maximum value and is decreasing until reaching the next commutation.
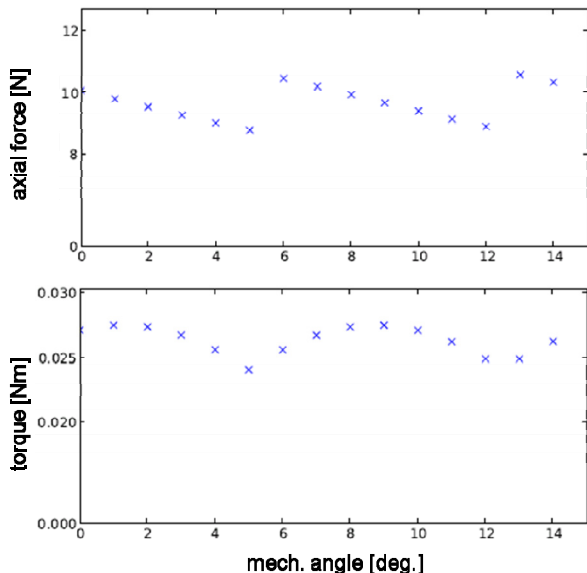
Fig. 5: Simulation results of axial force and tangential torque.

Between the commutation point the torque yields its maximum with 27 mNm. The peak to peak value of the simulated torque ripple in relation to the mean torque amounts to 14%. Due to the inertia of the rotor and the frequency of 2400 Hz at a nominal speed of 2500 rpm, it is expected that the ripple can not be proved by measurements. For the same reasons no negative effects on the drive performance is expected from the variations in the axial attracting force.

Over the whole simulated rotation the resulting torque exceeds the required torque. According to

$$T \sim \Theta_s \Theta_f \sin \varepsilon , \qquad (5)$$

the resulting torque T is proportional to the stator and excitation current linkage Θ_s and Θ_f as well as the angle ε between them. Due to the field oriented control with pulse current injection the torque is proportional to the stator current linkage as the open term of equation (5) is constant. For the loss calculation this relation is applied to determine the required stator current linkage for generating a torque of 12 mNm.

V. EXPERIMENTAL VALIDATION

The stator of the drive prototype is presented in Fig. 6. Due to manufacturing the possible copper fill factor is reduced from 60 to 52%. The resulting coil height is slightly increased to 5.1 mm. One coil consists of 4 layers with 9 turns each. In order to ensure a sufficient stability and to protect the coils the stator is molded in epoxy resin.

The test bench for the evaluation of the drive design is shown in Fig. 7. In the middle the permanent magnet rotor is directly attached to the shaft of an eddy current brake, realizing the required load. The stator is attached to a torque transducer and a three dimensional positioning system. In this assembly the axial hydrodynamic bearing is missing. The drive is supplied with a commercially available converter with integrated sensorless position detection and field oriented control. The set points for the converter as well as the control for the eddy current brake are realized via a rapid prototyping system. For controlling the speed an optical working tachometer is applied. Fig. 8 represents a measured speed torque characteristic. Due to the rolling resistance of the bearing of the eddy current brake shaft the torque rises linear with the speed up to the rated speed of 2500 rpm. When increasing the input further, the resulting torque is rising as

Fig. 6: Stator with winding of the drive prototype.

EHE2011 - 4th International Conference on Electromagnetic Fields, Health and Environment, Coimbra-Portugal, 26th-28th May 2011

EHE2011 - pohl
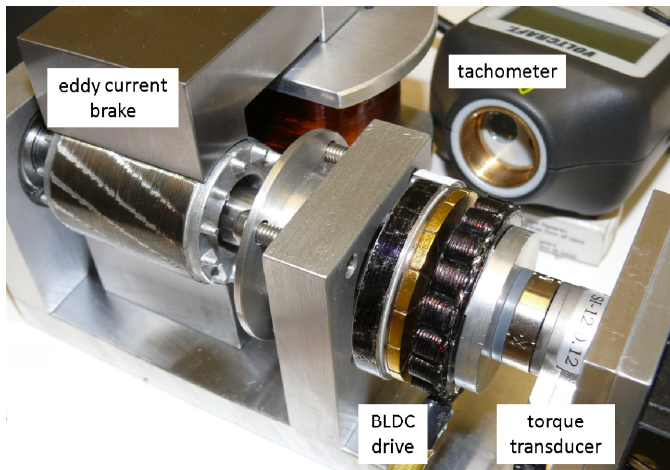
Fig. 7: Test bench for the validation of the drive design.

well, allowing for an overload capability.

For the nominal operating speed n_N of 2500 rpm and torque T_N of 12 mNm, the input power of the converter and the drive is measured with a power meter. The resulting mechanical output power can be calculated by applying

$$P_{mech} = 2 \cdot \pi \cdot n_N \cdot T_N .\qquad(6)$$

When dividing the mechanical output power by the measured input power, the overall efficiency as well as the drive efficiency can be calculated to 33% and 41% respectively.

The axial attracting force was proved by replacing the eddy current brake with a force sensor. Then the air gap width was varied via the three dimensional positioning system. According to TABLE 2 the resulting axial force is lower than expected. For this reason an operation with the axial hydrodynamic bearing is possible.

VI. SUMMARY & CONCLUSIONS

Cardiovascular diseases are the mayor cause of death in industrialized countries. The standard therapy heart transplant is limited due to the insufficient number of available donor heart. If some heart function is retaining, VADs are assisting in achieving a sufficient cardiac output. For the drive design this requirement is transferred to a torque of 12 mNm.
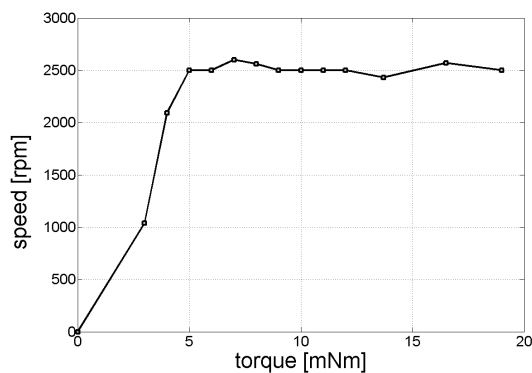
Fig. 8: Measured speed vs. torque characteristic.

TABLE 2: AXIAL FORCE VS. AIR GAP WIDTH

air gap width	axial force
1.5 mm	4.2 N
1.25 mm	6.6 N
1 mm	8.2 N
0.8 mm	9.8 N

Then the general design of a VAD and its BLDC drive is presented. In order to achieve a long durability and to limit the input power a passive and contactless axial hydrodynamic bearing is introduced. This bearing can only compensate axial forces of 9 N. In order to avoid blood damage caused by copper losses, they should be as low as possible. For this multiobjective drive design the DEA is applied, which is based on FE simulations due to occurring stray flux, a relative large air gap width and the rotational movement, causing reluctance forces. Because of a high amount of required FE simulations only the final drive design is validated by non linear simulations. The design results in a axial forces of 9 N and a torque 12 mNm at copper losses of 0.66W. The described measurements of the drive prototype proved its design.

The stator yoke is made of solid steel due to the axial flux flow through the stator teeth. Therefore the propagation of eddy currents, causing iron losses, is not prevented. As the copper losses are quite low and the drive efficiency only amount to 41%, the iron losses are expected to be significant. Therefore further simulations for their determination are required followed by a material study to reduce them. A high potential is seen in soft magnetic composite, which consist of isolated particles, reducing eddy currents. But the disadvantage of such material is its relative low saturation induction.

For the validation of the drive in VAD operation, the VAD is connected to a circulatory mock loop. Such a mock loop mainly consists of hydrostatic heads, representing the pressures of the human blood circuit. Again, the drive generated enough torque to provide the desired torque. This time the axial hydrodynamic bearing was included in the drive, but was not able to compensate the axial force of 9N. Therefore a redesign is required here.

VII. REFERENCES

[1] World-Health-Organization, "http://www.who.int/mediacentre/factsheets/," accessed Nov. 2010.

[2] J. G. Copeland, R. Smith, F. Arabia, P. E. Nolan, G. K. Sethi, P. H. Tsau, D. McClellan, and M. J. Slepian, "Cardiac replacement with a total artificial heart as a bridge to transplantation," *N Engl J Med*, vol. 351, pp. 859–867, August 2004.

[3] Andre Pohlmann, Marc Leßmann and Kay Hameyer, Comparative Study on Optimization Methods for a Motor-Drive of Artificial Hearts, in: Conference on Electric Machines and Systems, ICEMS, pages CD, KIEE, 2010.

[4] K. V. Price, R. M. Storn and J. A. Lampinen, "Differential Evolution - A Practical Approach to Global Optimization", 1st ed., *Springer*, 2005.

[5] U. K. Chakraborty, "Advances in Differential Evolution", *Springer*, 2008.

[6] K. Hameyer and R. Belmans: *Numerical modelling and design of electrical machines and drives*, Computational Mechanics Publications, WIT Press, Southampton 1999.

[7] Institute of Electrical Machines (IEM), RWTH Aachen University "www.iem.rwth-aachen.de", accessed May 2010.